Original article

MOLECULAR METABOLISM

Therapeutic effects of adropin on glucose tolerance and substrate utilization in diet-induced obese mice with insulin resistance

Su Gao [1], Ryan P. McMillan [2], Qingzhang Zhu [1], Gary D. Lopaschuk [4], Matthew W. Hulver [2], Andrew A. Butler [1,3,*]

ABSTRACT

Objective: The peptide hormone adropin regulates fuel selection preferences in skeletal muscle under fed and fasted conditions. Here, we investigated whether adropin treatment can ameliorate the dysregulation of fuel substrate metabolism, and improve aspects of glucose homeostasis in diet-induced obesity (DIO) with insulin resistance.

Methods: DIO C57BL/6 mice maintained on a 60% kcal fat diet received five intraperitoneal (i.p.) injections of the bioactive peptide adropin$^{34-76}$ (450 nmol/kg/i.p.). Following treatment, glucose tolerance and whole body insulin sensitivity were assessed and indirect calorimetry was employed to analyze whole body substrate oxidation preferences. Biochemical assays performed in skeletal muscle samples analyzed insulin signaling action and substrate oxidation.

Results: Adropin treatment improved glucose tolerance, enhanced insulin action and augmented metabolic flexibility towards glucose utilization. In muscle, adropin treatment increased insulin-induced Akt phosphorylation and cell-surface expression of GLUT4 suggesting sensitization of insulin signaling pathways. Reduced incomplete fatty acid oxidation and increased CoA/acetyl-CoA ratio suggested improved mitochondrial function. The underlying mechanisms appear to involve suppressions of carnitine palmitoyltransferase-1B (CPT-1B) and CD36, two key enzymes in fatty acid utilization. Adropin treatment activated pyruvate dehydrogenase (PDH), a rate-limiting enzyme in glucose oxidation, and down-regulated PDH kinase-4 (PDK-4) that inhibits PDH. Along with these changes, adropin treatment downregulated peroxisome proliferator-activated receptor-gamma coactivator-1α that regulates expression of *Cpt1b, Cd36* and *Pdk4*.

Conclusions: Adropin treatment of DIO mice enhances glucose tolerance, ameliorates insulin resistance and promotes preferential use of carbohydrate over fat in fuel selection. Skeletal muscle is a key organ in mediating adropin's whole-body effects, sensitizing insulin signaling pathways and altering fuel selection preference to favor glucose while suppressing fat oxidation.

Keywords Adropin; Glucose metabolism; Fatty acid metabolism; Insulin action; Metabolic flexibility; Mitochondrial function

1. INTRODUCTION

Adropin is a small peptide that has been linked to metabolic homeostasis and cardiovascular function [1–4]. High levels of expression of the *Energy Homeostasis* Associated (*Enho*) gene encoding adropin have been observed in the central nervous system, although widespread expressions in peripheral tissues such liver, cardiac and skeletal muscle, and endothelium have also been reported [4–6]. Adropin was originally proposed to be a secreted factor, with residues 1-33 encoding a secretory signal peptide [4]. A more recent study suggests that adropin might be a membrane-bound protein that interacts with the notch signaling pathway to modulate intercellular communications [5]. While the source and mechanism of release remains controversial, adropin immunoreactivity has nevertheless been reported by several laboratories to be present in plasma and sera of mouse, nonhuman primate and human [3,7–23]. Studies in mice suggest that the gene expression and the circulating levels of adropin are affected by dietary macronutrients and energy balance states [3,4,20,24,25].

The rapid regulation of adropin levels by nutritional and energy states points to potential roles for adropin in metabolic homeostasis. Indeed, early studies showed that transgenic overexpression of adropin or treatment using the putative secreted domain (adropin$^{34-76}$) improved glucose clearance, reduced fasting insulin and reversed dyslipidemia and the fatty liver phenotype in diet-induced obese C57BL/6 (DIO) mice [4]. In addition, our group observed evidence of insulin resistance in

[1]Department of Metabolism and Aging, Scripps Research Institute, Jupiter, FL, USA [2]Department of Human Nutrition, Foods and Exercise, Virginia Polytechnic Institute and State University, Blacksburg, VA, USA [3]Department of Pharmacological & Physiological Science, Saint Louis University School of Medicine, Saint Louis, MO, USA [4]Department of Pediatrics, Mazankowski Alberta Heart Institute, University of Alberta, Edmonton, AB, Canada

*Corresponding author. Pharmacological & Physiological Science, Saint Louis University School of Medicine, 1402 S Grand Blvd, St Louis, MO 63104, USA. Tel.: +1 314 977 6425; fax: +1 314 977 6410. E-mail: Butleraa@SLU.edu (A.A. Butler).

Received December 8, 2014 • Revision received January 6, 2015 • Accepted January 9, 2015 • Available online 17 January 2015

http://dx.doi.org/10.1016/j.molmet.2015.01.005

the adropin knockout mice [20]. Furthermore, we recently proposed that adropin regulates the preference for fuel selection in skeletal muscle in the feeding and fasting cycle [3]. We posited that increased release of adropin, such as in the fed state, activates pyruvate dehydrogenase (PDH) complex to increase glucose oxidation [3]. In parallel, adropin reduces muscle fatty acid oxidation (FAO) by inhibiting carnitine palmitoyltransferase-1B (CPT1B) [3], a key enzyme that transports fatty acids into muscle mitochondria for β-oxidation [26].

Dysregulation of glucose and fatty acid metabolism is a metabolic signature in the diet-induced obese (DIO) state [27]. In the DIO condition, glucose utilization is diminished and fatty acids are the predominant fuel source in muscle [27]. One mechanism explaining altered fuel selection preference involves the excessive FAO that inhibits pyruvate and glucose oxidation by the Randle cycle mechanism [28–31]. A growing body of evidence suggests that limiting excessive FAO in muscle plays a role in maintaining glucose homeostasis in DIO rodents [30–32]. As our data suggest that adropin is a physiological regulator of the oxidation of glucose and fatty acid, we speculated that adropin treatment would exert therapeutic roles in ameliorating the dysregulated fuel metabolism and glucose intolerance in DIO state. Indeed, recent evidence indicates that high-fat feeding results in muscle mitochondrial fatty acid overload and excessive β-oxidation, which has been proposed to contribute to the development of insulin resistance in DIO mice [30]. Furthermore, it has been suggested that inhibition of muscle FAO can alleviate insulin resistance in DIO mice [32]. Taking these observations together, we hypothesized that adropin treatment would enhance insulin actions in muscle of DIO mice. The current study investigated whether adropin treatment would impact substrate utilization, improve glucose homeostasis and ameliorate insulin resistance in the diet-induced obesity.

2. MATERIALS AND METHODS

2.1. Animal studies

Mouse experiments were approved by the Institutional Animal Care and Use Committees of the Scripps Research Institute (Jupiter, Florida). Male, lean or DIO C57BL/6 mice were purchased from the Jackson Laboratory (Bar Harbor, ME). Lean mice were maintained on low-fat diets (10–14% kcal fat). DIO mice were maintained on high fat diet (60% kcal fat) (Research Diets, New Brunswick, NJ). Mice were monitored daily after shipment until body weight became stabilized. Mice subjected to experimental procedures were 24-week old. Body composition was determined using a NMR spectroscopy analyzer (Bruker Minispec).

2.2. Adropin treatment

Adropin$^{34-76}$ was provided by Ipsen (Paris, France) or purchased from ChinaPeptides (Shanghai, China). The peptide was dissolved in 0.1% bovine serum albumin, and administered by intraperitoneal (i.p.) injection.

2.3. Glucose and insulin tolerance tests

The animal handling and injection protocols used for glucose tolerance test (GTT) (glucose, 2 mg/g fat-free mass) and insulin tolerance test (ITT) (Humulin, Eli Lilly, IN; insulin, 0.5 mU/g body weight) are shown in Figure 1. Blood glucose levels were monitored using OneTouch Blood Glucose Meters (LifeScan Europe, Switzerland) at the times indicated. Serum insulin levels were measured using an Ultrasensitive Mouse Insulin ELISA kit (Crystal Chem, Downers Grove, IL).

2.4. Whole body metabolic assessment

Oxygen consumption (VO_2), carbon dioxide production (VCO_2) and respiratory exchange ratio (RER; VCO_2/VO_2) were measured using a

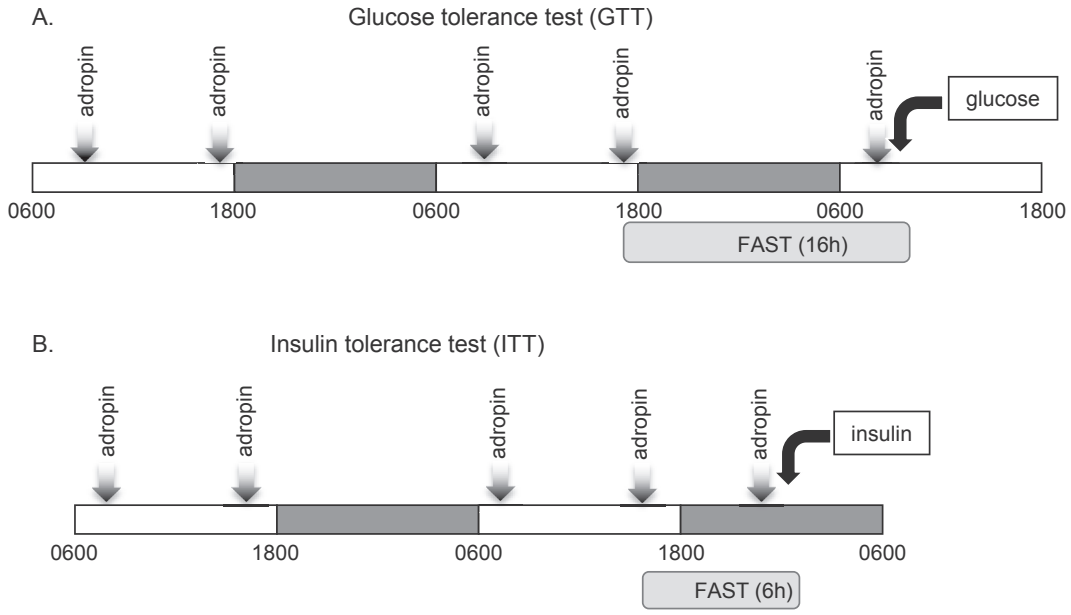

Figure 1: Schemes of the animal treatment for the assessments of glucose and insulin tolerance in DIO mice. DIO mice received five intraperitoneal (i.p.) injections of adropin$^{34-76}$ or vehicle over a 48 h period. A group of chow-fed lean mice included in the study received injections of vehicle. (A) Protocol for assessing the impact of adropin treatment on glucose tolerance. After the 4th injection of adropin or vehicle, food was removed and the mice fasted overnight. The mice received a 5th injection the next morning; one hour later, baseline blood glucose levels were determined (t = 0); mice then received an i.p. injection of glucose (2 mg/g fat free mass). Glucose levels were then determined at 15 min intervals. (B) Protocol for assessing the impact of adropin treatment on insulin tolerance. DIO and the lean control mice received five intraperitoneal (i.p.) injections of adropin$^{34-76}$ or vehicle. One hour after the 5th injection, the mice that had been fasted for 6 h were given an i.p. injection of insulin (0.5 mU/g body weight).

comprehensive laboratory animal monitoring system (CLAMS; Columbus Instruments, Columbus, OH). Heat production (kcal/h/mouse) was calculated using the formula: (3.815 + 1.232*RER)* VO_2. The proportions of heat derived from carbohydrate and fat oxidation were estimated based on heat production and RER [33].

2.5. Western blotting analysis

Standard immunoprecipitation and immunoblotting procedures were performed according to the protocols detailed by Cell Signaling Technology (Danvers, MA) and Invitrogen (Carlsbad, CA), respectively. The antibodies to detect phospho-Akt (S^{473}), Akt, phospho-AS160 (T^{642}), insulin receptor substrate 1 (IRS1), phospho-Tyrosine (pY), phospho-c Jun N-terminal kinase (JNK) (T^{183}/Y^{185}), p85 subunit of PI-3 kinase, JNK, phospho-inhibitor kappa B kinase (IKK) α/β ($S^{176/180}$), IKKβ, pyruvate dehydrogenase (PDH) E1α subunit, GLUT4, Na-K ATPase, glyceraldehyde 3-phosphate dehydrogenase (GAPDH) and conformation-specific anti-Rabbit IgG were from Cell Signaling Technology (Danvers, MA). The PTEN and SIRT3 antibodies are from Santa Cruz Biotechnology (Dallas, Texas). The anti-PDK2 Ab is from Abcam (Cambridge, MA). The AS160 Ab was from both Cell Signaling Technology and Millipore (Billerica, MA). The CD36 Ab was from Novus Biologicals (Littleton, CO). The anti-PDH-E1α (pSer232) Ab was from Millipore. The antibodies to detect PGC-1α, PDK4, and acetylated-Lysine (Ac-K) were described previously [3]. GAPDH was used as the loading control in whole cell lysate analysis. Densitometry was performed with the Scion image software (Frederick, MD).

2.6. Subcellular fractionation

To measure GLUT4 and CD36 protein contents in the cell surface, muscle tissues were subject to the subcellular fractionation procedures that were detailed in [34]. In brief, fragments of the quadriceps muscle were minced and homogenized in 2 volumes of STE buffer [0.32M sucrose, 20 mM Tris-HCL (pH 7.4), 2 mM EDTA] with protease and phosphatase inhibitors (Roche Life Science, Indianapolis, IN). The homogenates were centrifuged at 1,000 g, and the pellet was suspended in Triton buffer [1% Triton X-100, 20 mM Tris-HCL (pH7.4), 150 mM NaCl, 200 mM EDTA] with protease and phosphatase inhibitors (Roche Life Science, Indianapolis, IN). The suspension was centrifuged at 15,000 g to separate the nuclear fraction. The supernatant was centrifuged at 100,000 g (Beckman Coulter Optima Ultracentrifuge) to obtain a pellet that was suspended in the STE buffer plus 1% Nonidet P-40, and centrifuged at 100,000 g to obtain the membrane fraction. All procedures were performed at 4 °C. The GLUT4 and CD36 protein were then detected with the respective antibodies, with Na-K ATPase serving as the loading control of cell surface (plasma membrane) fraction [32].

2.7. Fatty acid oxidation

FAO was measured using whole muscle homogenates as described before [3,35]. [U-^{14}C] palmitic acid was used as the substrate. Skeletal muscle samples were homogenized in the buffer containing 0.25M Sucrose, 1 mM EDTA, 0.01M Tris-HCL (pH 7.4), and 2 mM ATP. The reaction was initiated by adding a reaction mixture containing the [U-^{14}C] palmitic acid into the muscle homogenate. The reaction was incubated in a trapping device at 37 °C for 1 h before 70% perchloric acid was added to trap CO_2 production. The trapping mixture was further incubated under room temperature for 1 h before NaOH was added. A portion of the mixture containing the trapped CO_2 was used for scintillation counting. The acidified portion that constitutes the acid soluble metabolites (ASM) was collected, and incubated overnight under 4 °C. Following the overnight incubation, the ASM was centrifuged at 15,000 g, and the supernatant was used for scintillation counting. The $^{14}CO_2$ production from the labeled palmitate indicates complete oxidation, and the production of ^{14}C-labeled ASM indicates incomplete oxidation.

2.8. CPT1 activity assay

CPT-1 activity was measured using freshly prepared mitochondria as described previously [3,36]. In brief, the muscle samples were homogenized in buffer B (250 mM Sucrose, 10 mM Tris-HCl (pH 7.4) and 1 mM EDTA). The muscle homogenate was centrifuged at 600 g, and the resultant supernatant was centrifuged at 12,000 g. The pellet was suspended in buffer B, centrifuged at 8,000 g, washed, and finally resuspended in buffer B. The suspension was enriched in mitochondria, and was used for the CPT-1 activity assay. The reaction was initiated by adding the mitochondria sample to the assay mixture containing L-[^{14}C-*Me*] carnitine and palmitoyl-CoA as substrates. The reaction was incubated at 30 °C for 5 min, and terminated by the addition of 1.2N HCl. Extractions of the product of the reaction, palmitoyl-^{14}C-carnitine, were conducted by adding water-saturated butanol. The mixture was centrifuged at 1,000 g, and the upper phase was removed, mixed with H_2O, and centrifuged at 2,000 g. A portion of the upper phase was then used for scintillation counting.

2.9. Pyruvate dehydrogenase (PDH) activity assay

The mice were euthanized within two hours after the last injection, and the muscle tissues were freeze-clamped and flash-frozen in liquid nitrogen. The PDH activity from whole muscle lysate was measured by use of colorimetric microplate assay kit from Mitosciences (Eugene, OR) [37], following the manufacturer's protocol. In brief, PDH proteins from whole cellular lysate were immunocaptured on a microplate. A reaction mixture containing pyruvate and NAD^+ is then added to the plate. The readout is the rate of production of NADH, which was further coupled to the reduction of a reporter dye to yield a colored reaction product. The formation of the colored product was then monitored on a spectrophotometer, and the PDH activity was calculated by use of the rate of the change in optical density. Preliminary study showed a 50% decrease in the native PDH activity in the fasted muscle extract, which validates the assay. In addition, the PDH activity levels in the current study are in the similar range as in another report using the same kit [37].

2.10. Glycogen and triacylglycerol assay

Glycogen and triacylglycerol were measured by use of the Glycogen Assay Kit from Abcam (Cambridge, MA) and the Triglyceride Colorimetric Assay Kit from Cayman (Ann Arbor, MI), respectively, following the manufacturer's protocols.

2.11. Real-time PCR

The extraction of the total RNA from muscle samples was performed by use of the RNeasy Mini Kit from Qiagen (Valencia, CA). cDNA was synthesized using the high capacity cDNA reverse transcription kit from Applied Biosystems (Carlsbad, CA). PCR was conducted using a 7900 Fast Real-time PCR system, following the instructions from the TaqMan Gene Expression Assays (Applied Biosystems). The message levels of Gapdh were used as the loading control.

2.12. Metabolic profiling

Metabolomics analysis of the muscle samples was performed by Metabolon (Durham, NC). The levels of long-chain acyl-CoA, ceramide and malonyl-CoA were measured as reported before [32].

2.13. Statistical analysis

All data are presented as mean ± SEM. Unless otherwise noted, Student *t*-test or ANOVA followed by multiple comparison tests (Neuman-Keuls) was used to evaluate the statistical significance. A value of $P < 0.05$ is defined as statistically significant.

3. RESULTS

3.1. Adropin treatment improved glucose tolerance in DIO mice

To confirm that adropin$^{34\text{-}76}$ therapy improves glucose tolerance, we adhered to the treatment protocol that was shown previously to improve glucose tolerance [4]. We administered five intraperitoneal (i.p.) injections of adropin$^{34\text{-}76}$ (450 nmol/kg/i.p.) to DIO mice over 2–3 days; control DIO and lean mice were treated with the vehicle (Figure 1A). Injections of adropin$^{34\text{-}76}$ at this dose and duration did not alter body weight (Figure 2A), thus excluding potential effects of weight change on glucose tolerance. In the experiment examining glucose tolerance, the mice were fasted overnight, and a bolus intraperitoneal injection of glucose was administered at 1 h after the last injection of adropin$^{34\text{-}76}$ (Figure 1A). Blood glucose levels were then monitored in the following 90 min. The vehicle-treated DIO mice were glucose intolerant compared to the lean mice, and adropin treatment significantly improved glucose tolerance in DIO mice (Figure 2B). Serum insulin levels were also measured 90 min post-glucose injection, with adropin-treated DIO mice exhibiting levels that were lower relative to the vehicle-treated DIO mice (Figure 2C). We next assessed whether adropin treatment would improve whole body insulin action by performing insulin tolerance test (ITT) in mice fasted for 6 h (Figure 1B). DIO mice treated with adropin exhibited lower blood glucose levels, while the effect of insulin to lower blood glucose was enhanced relative to DIO controls (Figure 2D). Collectively, these data suggest that treating DIO mice with the adropin$^{34\text{-}76}$ peptide was effective at enhancing glucose tolerance and alleviating whole-body insulin resistance.

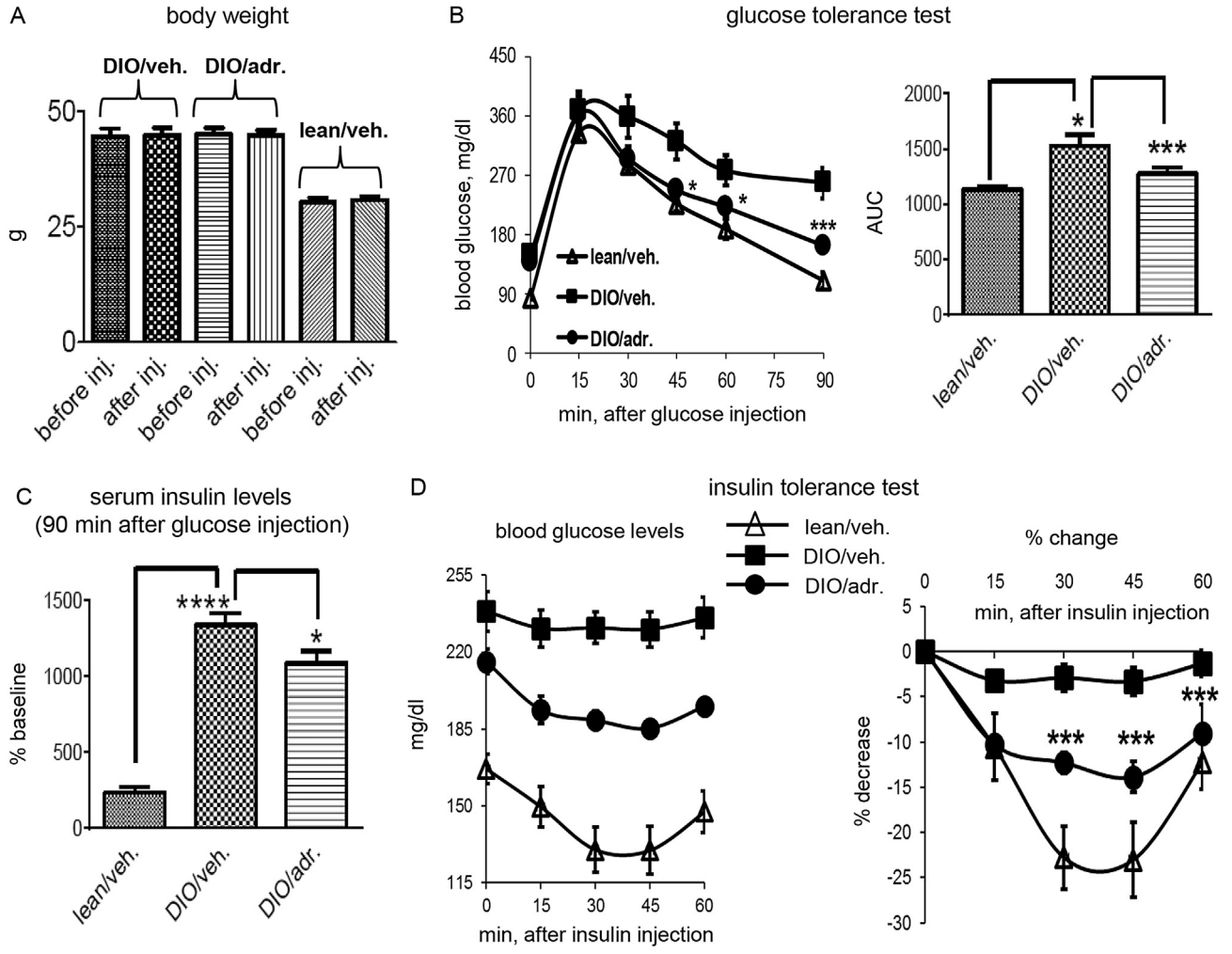

Figure 2: Treatment of DIO mice with adropin$^{34\text{-}76}$ enhances glucose tolerance and ameliorates insulin resistance without affecting body weight. (A) Body weights before the first injection and after the fifth injection were compared (n = 5). (B) Effect of adropin treatment on glucose tolerance. Following glucose injection, blood glucose levels were monitored at regular intervals for 90 min (n = 7–8). *: DIO/adr. vs. DIO/veh., $P < 0.05$; ***: DIO/adr. vs. DIO/veh., $P < 0.001$. The *right panel* shows the area under the curve (AUC) calculated for the glucose excursion curve. *: DIO/veh. vs. lean/veh., $P < 0.05$; ***: DIO/adr. vs. DIO/veh., $P < 0.001$. (C) Glucose-induced changes in serum insulin levels following adropin treatment. Serum samples were collected from two experiments, and the values of insulin levels at 90 min after glucose injection are expressed as a percentage of the basal level (i.e., fasting values before glucose injection) of the lean controls (0.45 ng/ml). ****: DIO/veh. vs. lean/veh., $P < 0.0001$; *: DIO/adr. vs. DIO/veh., $P < 0.05$. (D) Effect of adropin treatment on whole body insulin sensitivity. Blood glucose levels were monitored at 15-min interval for 60 min (n = 6–9) after an injection of insulin. The right panel shows the percent decline (% decrease) in blood glucose following insulin injection. ***: DIO/adr. vs. DIO/veh., $P < 0.001$.

3.2. Adropin treatment enhanced glucose oxidation and metabolic flexibility

Our previous results suggest that adropin is involved in the physiological control of fuel selection [3]. In the current study, we conducted indirect calorimetry to assess whether adropin treatment, associating with the enhancement of glucose and insulin tolerance, would impact fuel utilization in DIO mice. The protocol used for this experiment was similar to that used to investigate glucose tolerance (Figure 1A). The acclimated DIO mice received five injections of adropin$^{34\text{-}76}$, and then a bolus of a mixture consisting of insulin and glucose was given to the mice.

Prior to the insulin/glucose challenge, adropin injections induced a subtle but significant increase in the RER (Figure 3A, "pre-INS/GLU"), suggesting preferential oxidation of carbohydrate over fat. The injection of insulin/glucose induced increases in RER in both the vehicle and the adropin-treated mice, and the increase ("delta") was more pronounced in the adropin-pretreated mice than in the vehicle-pretreated controls (Figure 3A, "post-INS/GLU"). Total energy expenditure indicated by heat production was not affected by adropin treatment (Figure 3B, "pre-INS/GLU"). When the individual levels of substrate oxidation were calculated, adropin-treated mice showed a trend ($P = 0.07$) of an increase in glucose oxidation and a decrease ($P = 0.1$) in fatty acid oxidation (Figure 3C and D, "pre-INS/GLU"). Injection of the insulin/glucose mixture induced increases in glucose oxidation in both the vehicle- and adropin-treated mice, and the adropin-pretreated mice exhibited a greater response (to insulin/glucose) than the vehicle-pretreated animals (Figure 3C). In parallel with the enhanced shift towards glucose oxidation, a decline in fatty acid oxidation following insulin/glucose injection was also observed following adropin$^{34\text{-}76}$ treatment (Figure 3D, "post-INS/GLU"). Taken together, the data suggest that adropin$^{34\text{-}76}$ therapy enhances glucose oxidation and ameliorates metabolic inflexibility of utilizing glucose in obese and insulin resistant mice.

3.3. Adropin treatment enhanced insulin signaling pathways in muscle

We next investigated whether adropin$^{34\text{-}76}$ treatment would improve insulin signaling actions in skeletal muscle. The mice were treated employing a protocol similar to that used for the ITT test (Figure 1B). DIO and the lean control mice received five injections of adropin or its vehicle, and a bolus of insulin or saline was given to the mice. Akt is a key component in insulin intracellular signaling pathways; most studies support an important role for Akt in insulin-stimulated glucose uptake in muscle [38–40]. In our studies, the insulin-induced increase in Akt phosphorylation, an indicator of kinase activity, was blunted in the muscle of DIO mice, as compared to the lean mice (Figure 4A) [41]. DIO mice treated with adropin exhibited an augmented response relative to DIO mice treated with the vehicle, suggesting an enhanced insulin signaling through Akt (Figure 4A). Increased phosphorylation of Akt substrate 160 (AS160) mediates the

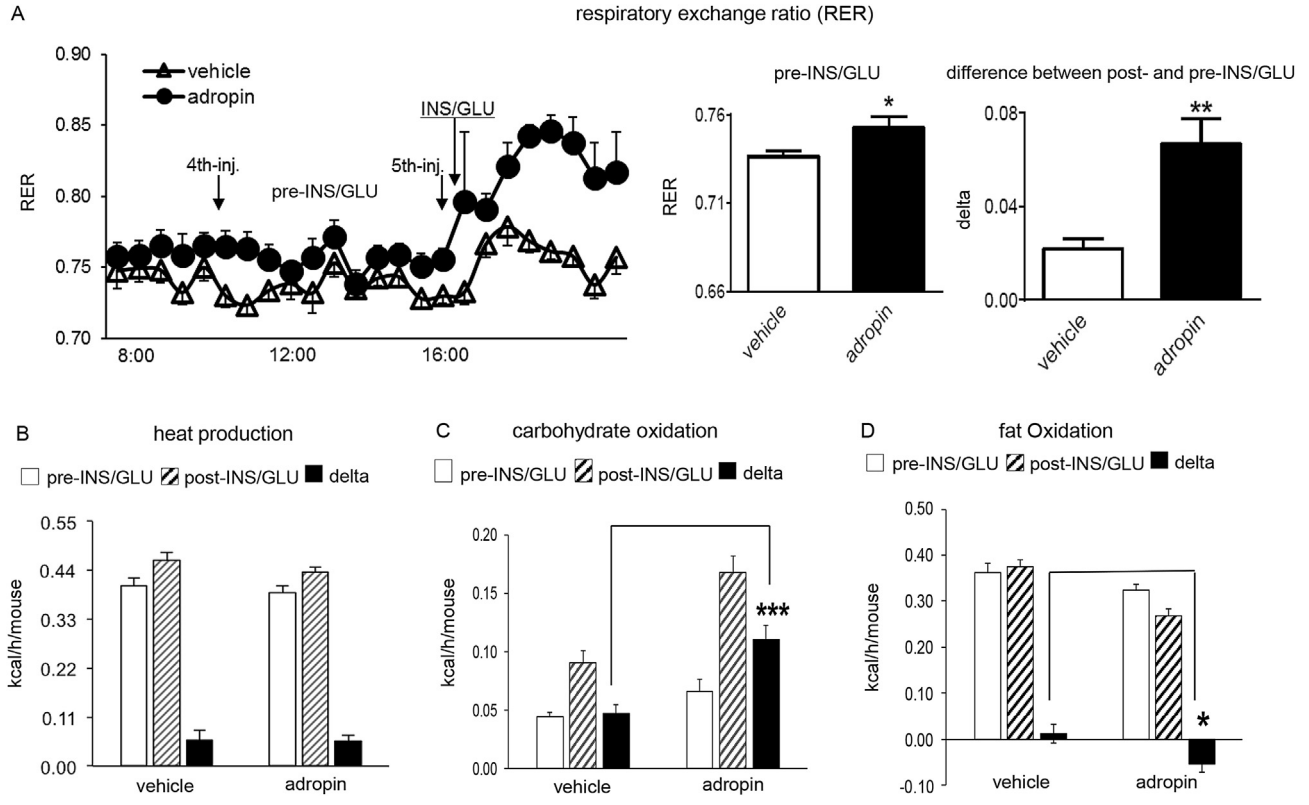

Figure 3: Adropin treatment increases carbohydrate oxidation and enhances metabolic flexibility towards glucose oxidation in DIO mice. DIO mice received 5 injections of adropin or vehicle ($n = 8$) prior to injection of a bolus of insulin (2 mU/g) and glucose (2 mg/g) (INS/GLU); the mice had been fasted for 16 h prior to the injection of INS/GLU. (A) The respiratory exchange ratio (RER) for the time preceding and following the insulin/glucose injection. The left panel of curves shows the individual RER values along the injections. The averaged values for each animal between the 4th and 5th injection are designated as "Pre-INS/GLU". Values averaged after the 5th injection were designated as "Post-INS/GLU". The differences (delta) between the pre-injection average and the post-injection average, i.e., "Post-INS/GLU" minus "Pre-INS/GLU", were then calculated. (B) Heat production (kcal/h) for the "Pre-INS/GLU" and the "Post-INS/GLU" period defined in (A), and the change (delta) of heat productions ("Post" minus "Pre") were calculated. The corresponding carbohydrate oxidation levels (C) and fat oxidation levels (D) were calculated. *, $P < 0.05$; **, $P < 0.01$; ***, $P < 0.001$.

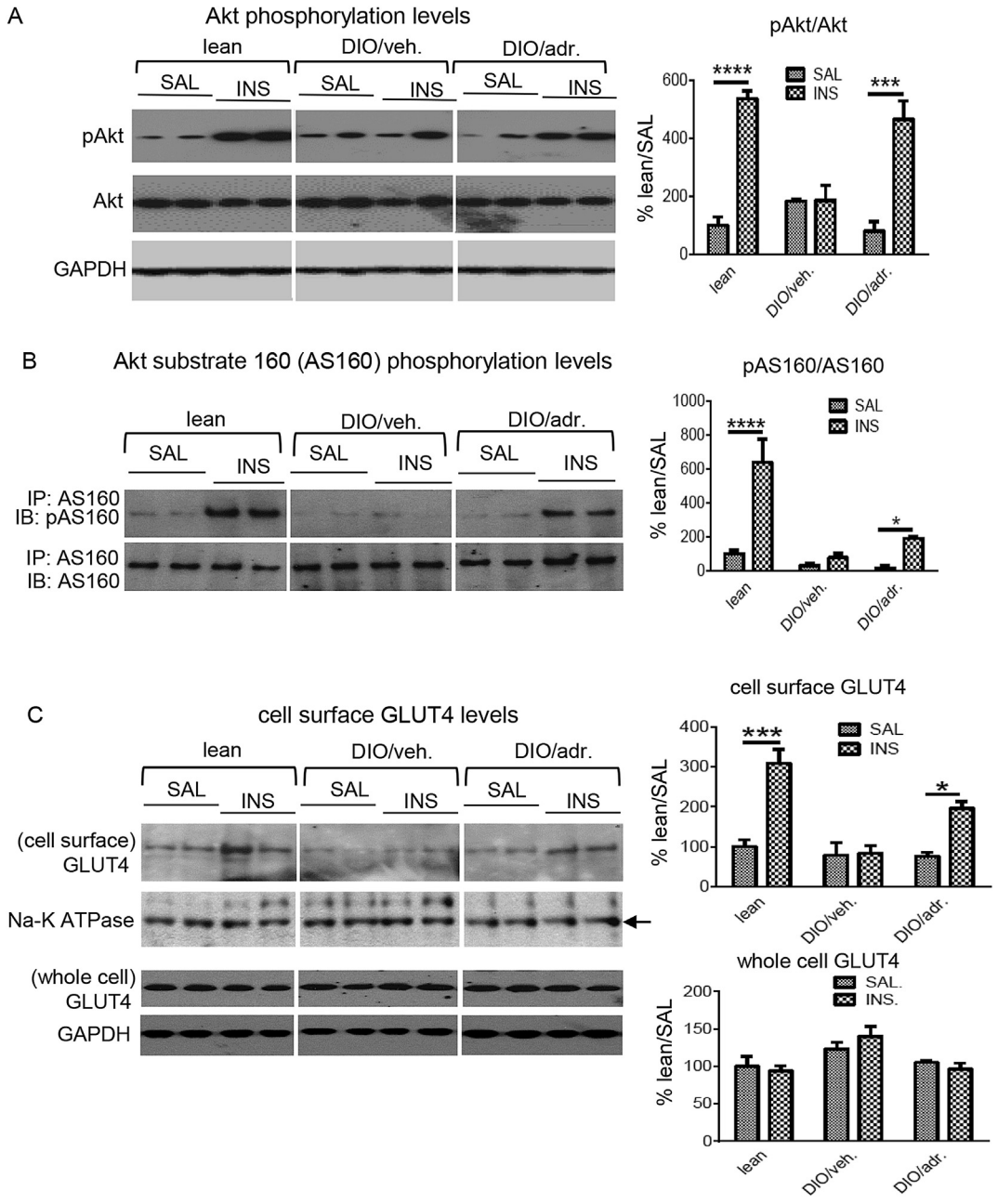

Figure 4: Adropin treatment enhances insulin-signaling actions in muscle of DIO mice. DIO and lean control mice received five injections of adropin$^{34\text{-}76}$ or the vehicle, and were fasted for 6 h, with a final adropin injection administered 5 h into the fast. The mice then received i.p. injections of insulin (INS, 5 mU/g) or saline (SAL). Muscle tissue was freeze clamped and flash frozen in liquid nitrogen 10 min after the injection of insulin or saline. (A) The muscle samples were divided into two subgroups using two sets of gels ($n = 4–8$). The representative blots from one set of gels were presented, showing phospho-Akt (pAkt-S^{473}) and total Akt ($n = 2–4$). GAPDH was used as the loading control. The level of the pAkt or total Akt was normalized to the corresponding GAPDH, and the ratios of the normalized pAkt to the normalized Akt were presented. (B) The Ab against Akt substrate 160 (AS160) was used to immunoprecipitate AS160 protein from whole muscle lysate. The immunoprecipitates were probed with a phospho-AS160 (pAS160-T^{642}) Ab and AS160 Ab ($n = 3–5$). (C) GLUT4 contents in the subcellular fraction consisting mainly of cell surface were detected by Western blotting, and Na-K ATPase was used as the loading control (two muscle tissues were pooled; $n = 2–3$). In parallel, the GLUT4 protein levels in whole muscle lysate were shown ($n = 3–4$). In all blots, two representatives from individual groups in the same gel are presented. *, $P < 0.05$; ***, $P < 0.001$; ****, $P < 0.0001$.

effect of Akt on insulin-stimulated glucose uptake [42,43]. Consistent with previous data [44], insulin-stimulated AS160 phosphorylation (Thr642) was reduced in DIO muscle (Figure 4B). Adropin treatment partially restored the response to insulin injection (Figure 4B). The GLUT4 transporter lies downstream of AS160 action, and is recruited to cell surface following insulin stimulation [45]. In the current study, adropin treatment enhanced insulin-induced cell surface expression of GLUT4 without altering the whole cell level (Figure 4C). As the recruitment of GLUT4 to cell surface plays an essential role in mediating insulin-stimulated glucose uptake [45], our results suggest adropin treatment has the potential to promote insulin-induced glucose uptake in muscle.

We also assessed the responses of Akt upstream components including insulin receptor substrate-1 (IRS1) and phosphatidylinositide-3 kinase (PI3K) [46]. In lean mice, insulin induced tyrosine phosphorylation of IRS1, and increased the level of IRS1-associated p85 subunit of PI3K (Figure S1A) [41,47]. Compared to lean muscle, these increases were diminished in muscle of DIO mice (Figure S1A) [41,47]. Unexpectedly, adropin pre-treatment did not restore the diminished responses of IRS1 and PI3K despite enhancing Akt signaling actions (Figure S1A and Figure 4A). These data indicate that adropin treatment selectively enhanced the distal insulin signaling pathways in DIO mouse muscle. PI3K action induces Akt phosphorylation through producing phosphatidylinositol-3,4,5-trisphosphate (PIP_3), and PIP_3 is dephosphorylated by phosphatase and tensin homologue (PTEN) leading to inhibition of Akt signaling [48]. In our studies, the protein and message levels of PTEN in muscle of DIO mice were downregulated by adropin treatment (Figure S1B), which could lead to elevation of PIP_3 level and promote Akt phosphorylation in response to insulin challenge.

AMP-activated protein kinase (AMPK) can phosphorylate AS160 independent of Akt, contributing to insulin-independent glucose uptake in skeletal muscle [44]. We measured the phosphorylation levels of AMPK and acetyl-CoA carboxylase (ACC), surrogate makers of AMPK activity, and found no significant changes in these levels following adropin treatment (Figure S1C). This suggests that AMPK is not involved in adropin's metabolic effects in muscle of DIO mice, consistent with our previous observations [3].

3.4. Adropin treatment reduced incomplete fatty acid oxidation (FAO)

Prolonged high fat diet feeding has been shown to cause mitochondrial fatty acid overload in muscle, resulting in the buildup of incomplete oxidation products [30]. Confirming this argument, our data demonstrated elevated levels of acid soluble metabolites (ASM) in muscle lysates, which indicates the accumulation of incomplete FAO products (Figure 5A). Adropin$^{34\text{-}76}$ treatment reduced the increased ASM level (Figure 5A), suggesting that adropin action curtailed incomplete FAO promoted by high-fat diet feeding. Concomitantly, there were no changes in the level of CO_2 production in response to adropin injection (Figure 5B), indicating that complete FAO was not affected (by adropin). The overall FAO level was also calculated, which showed a decrease following adropin treatment as compared with the vehicle-treated DIO mice (Figure 5C).

Similar to what was previously observed in lean mice [3], adropin treatment reduced CPT1 activity (Figure 5D) and *Cpt1b* expression (Figure 5E) in the muscle of DIO mice. The excessive mitochondrial uptake of fatty acid and the subsequent β-oxidation can lead to sequestration of free CoA into acetyl-CoA (the end product of β-oxidation), which in turn reduces the CoA/acetyl-CoA ratio [30,49]. In

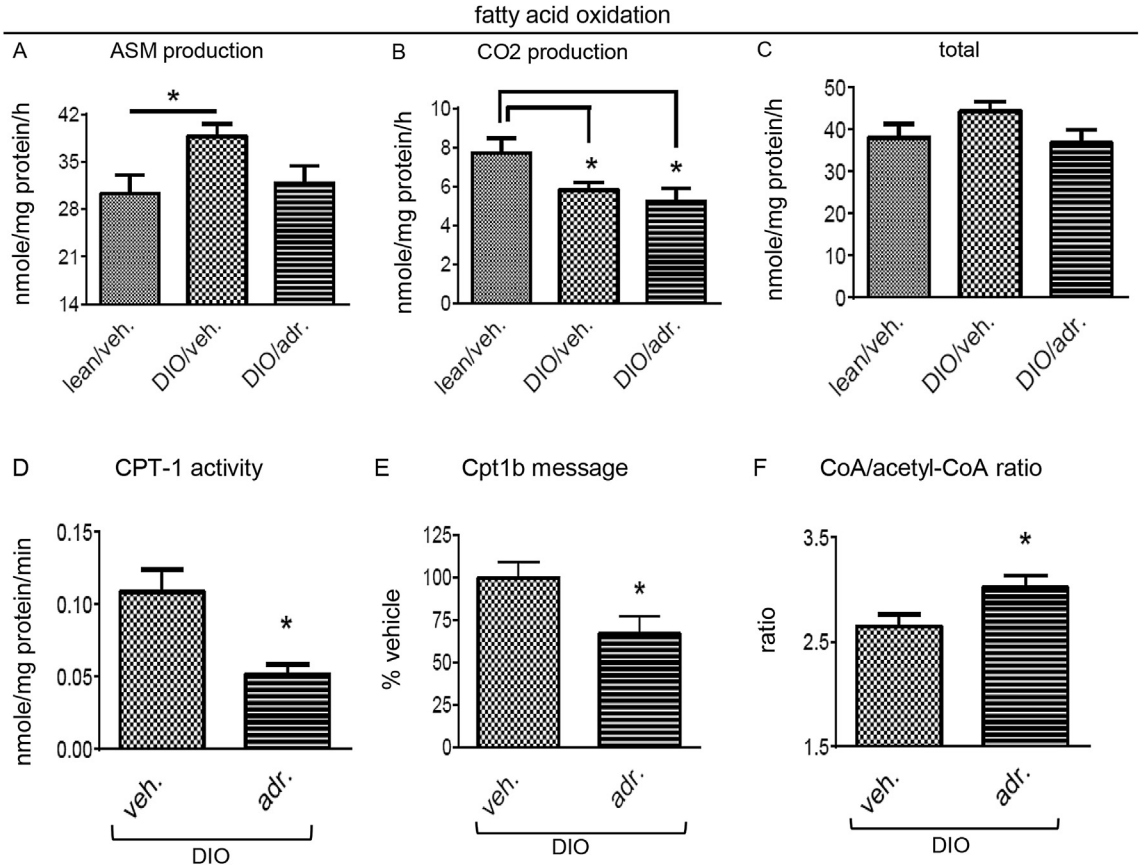

Figure 5: Adropin treatment of DIO mice reduced incomplete oxidation of fatty acid and reduced CPT1 activity in muscle. Whole muscle lysates were used for the measurement of the production of acid soluble metabolites (ASM), indicating incomplete oxidation (A), and the production of CO_2, indicating complete oxidation (B). (C) Total fatty acid oxidation (FAO) was calculated as the sum of the production of ASM and CO_2 ($n = 7$). (D) CPT-1 activities in isolated muscle mitochondria of vehicle- and adropin-treated DIO mice ($n = 4$). (E) Muscle Cpt1b message levels in vehicle- and adropin-treated DIO mice ($n = 6$). (F) Free CoA and acetyl-CoA levels in muscle of vehicle- and adropin-treated DIO mice were measured; the CoA to acetyl-CoA ratio (CoA/acetyl-CoA) is shown ($n = 5–6$). *, $P < 0.05$.

our studies, adropin treatment increased the CoA/acetyl-CoA ratio in DIO muscle (Figure 5F), which would be accounted for by the inhibitory effect of adropin treatment on CPT-1-mediated mitochondrial fatty acid uptake.

3.5. Adropin treatment increased glucose utilization in skeletal muscle of DIO mice

In lean mice, an increase in adropin levels upon feeding activates pyruvate dehydrogenase (PDH), a rate-limiting enzyme in the glucose oxidation pathway [3,50]. Consistent with previous reports [51], DIO mice exhibited reduced native PDH activity (Figure 6A). Importantly, adropin$^{34\text{-}76}$ treatment restored the native PDH activity to the levels observed in lean controls without changing total activity (Figure 6A).

Reversible phosphorylation is a critical mechanism underlying the regulation of PDH activity, with phosphorylation of specific serine residues in the E1α subunit inhibiting the enzymatic activity [49]. Consistent with the results of PDH activity assay, adropin treatment decreased the phosphorylation level of a key serine residue (Ser^{232}) of the E1α subunit (Figure 6B). In addition to phosphorylation, acetylation adds another layer of regulation of PDH activity [37]. Recent evidence demonstrates that in muscle, hyperacetylation of PDH E1α is associated with inhibition of PDH activity [37]. We therefore measured the acetylation level of PDH E1α, and observed a decrease following adropin treatment (Figure 6B). It is expected that this hypoacetylation would contribute to the adropin-induced activation of PDH. SIRT3 is a primary NAD^+ dependent deacetylase in the mitochondrion [52], and the E1α subunit of PDH is a substrate of SIRT3 [37]. We then investigated whether adropin treatment would impact SIRT3, thus leading to the altered acetylation level of PDH E1α subunit. The expression of SIRT3 protein is regulated by diet signals, and the level in muscle is reduced by high-fat diet feeding (Figure S2A) [53]. Following adropin treatment, the reduced level of SIRT3 protein in DIO mice was not affected (Figure S2A), which indicates that adropin may affect SIRT3 activity through mechanisms other than altering protein abundance.

In muscle, PDK-4 is a major PDK isoform that phosphorylates the serine residues of the E1α subunit to suppress PDH activity [49,54]. Altered gene expression is a common mechanism regulating PDK-4 activity [51,55]. Our results first confirmed the previous finding of

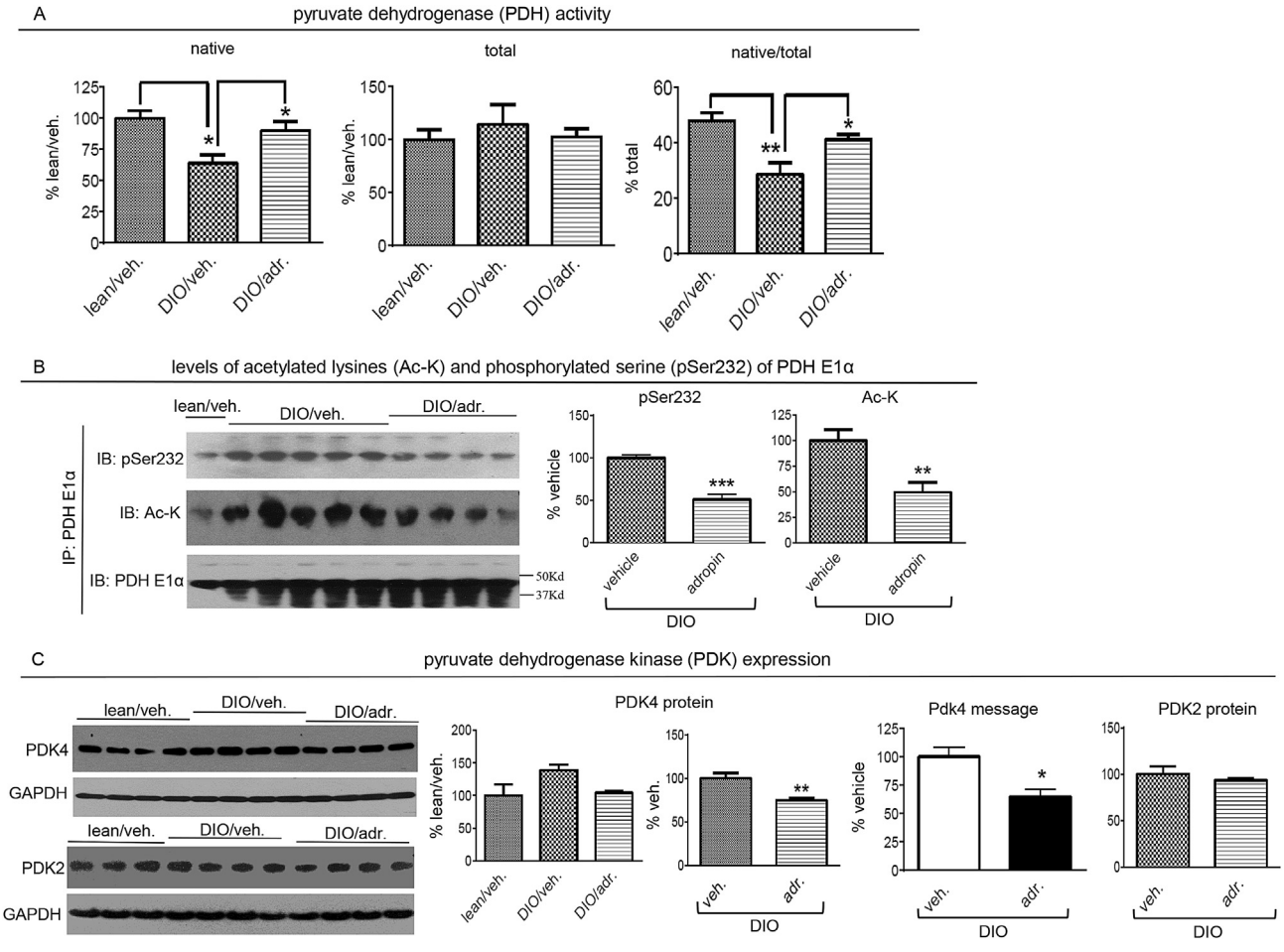

Figure 6: Adropin treatment increased pyruvate dehydrogenase (PDH) activity, and decreased PDK-4 expressions, in the muscle from DIO mice. (A) PDH activity. The activity in whole muscle lysate in the presence of phosphatase inhibitors and ATP-depleting system is designated as "native activity". The activity following phosphatase treatment is designated as "total activity". The ratio of the native activity to total activity was then calculated. (B) The PDH E1α subunit was immunoprecipitated. The immunoprecipitates were used for detections of phospho-Ser232 (pS^{232}), acetylated lysine (Ac-K) and total E1α (DIO group, n = 4–5). A conformation-specific anti-IgG antibody that only recognizes native IgG was used to detect the proteins. The molecular weight of the E1α subunit is 43Kda. (C) The levels of PDK4 protein (n = 4), PDK4 message (n = 5) and PDK2 protein (n = 3–4). *, $P < 0.05$; **, $P < 0.01$; ***, $P < 0.001$.

the increased PDK4 protein in DIO muscle [51], and further showed that adropin treatment reduced the levels of PDK4 message and protein (Figure 6C). In parallel with downregulating PDK-4 expression, adropin treatment did not affect the protein level of PDK-2 (Figure 6C) that is another isoform expressed in muscle [56]. Thus, adropin action appears to selectively impact PDK-4 expression in DIO mouse muscle, which is consistent with adropin's isoform-selective effect on PDK previously observed in lean mice [3].

Elevated levels of pyruvate oxidation can inhibit FAO at the level of CPT-1, which is in part due to the increased production of pyruvate-derived malonyl-CoA [29]. Following adropin treatment, malonyl-CoA level in DIO muscle was not altered (Figure S2), suggesting that adropin-induced FAO is not secondary to PDH activation.

We next investigated whether adropin treatment affects non-oxidative glucose disposal pathways including glycolysis and glycogen synthesis. Metabolic profiling analysis demonstrated that the levels of 2-phosphoglycerate (an intermediate in glycolysis) and lactate (end product of glycolysis) were increased following adropin treatment (Supplementary Data, Table 1), which indicates adropin treatment may increase glycolytic flux. Furthermore, adropin treatment partially restored glycogen level in DIO muscle to that observed in the lean mice (Figure S3). In addition, adropin-treated mice also had increased levels of mannose and fructose in muscle (Supplementary Data, Table 1), which may originate from the increased utilization of sucrose contained in the high-fat diet. Taken together, our data suggest that adropin actions increases glucose flux in DIO muscle through both oxidative and non-oxidative pathways.

3.6. Adropin treatment reduced PGC-1α in DIO muscle

The transcriptional co-activator PGC-1α regulates the expression of genes involved in oxidative metabolism [57], and appears to be involved in the adropin-mediated physiological control of fuel selection [3]. DIO mice treated with adropin$^{34-76}$ exhibited reduced message and protein levels of PGC-1α (Figure 7), which may account for the suppressions of Cpt1b and Pdk4 that are downstream targets of PGC-1α [58–61]. We previously reported that adropin-induced changes in PGC-1α did not alter mitochondrial content and oxidative capacity [3]. Here, we presented similar results in muscle of DIO mice. Citrate synthase activity, a marker of mitochondrial content [62], expression of mitochondrial transcription factor A (mtTfa) that is proportional to mtDNA copy number [63], and mitochondrial oxygen consumption indicating oxidative capacity were not altered by adropin treatment (Figure S4A, S4B and S4C).

3.7. Adropin treatment did not increase levels of fatty acid intermediates in muscle

Suppressing CPT-1 activity might cause intracellular accumulation of lipids that could also affect insulin sensitivity [64]. The levels of long-chain acyl-CoA's, ceramide and triacylglycerol were all increased in DIO muscle compared to lean mice; however, adropin$^{34-76}$ treatment did not affect their levels (Figure 8A). Diacylglycerol levels were also not altered by adropin treatment (fold change: adropin/vehicle $= 1.01$, $P > 0.05$).

Inhibition of CPT-1B can induce compensatory suppression of CD36 [32] that is a major fatty acid transporter in muscle [65]. Indeed, the mRNA and whole cellular protein levels of Cd36 were decreased by adropin treatment (Figure 8D). These data demonstrate that adropin actions down regulated Cd36 gene expression. In parallel with the downregulation of expression, the CD36 protein level in the cell surface was also decreased by adropin treatment, which indicates that adropin treatment may reduce muscle fatty acid uptake. It further follows that the potential reduced fatty acid uptake prevents the increases in intramuscular lipid levels resulting from the inhibition of CPT-1 activity by adropin treatment.

Cd36-deficient mice exhibit increased level of plasma free fatty acids [65]. In spite of the reduced levels of CD36 in muscle, adropin treatment did not affect the plasma levels of fatty acid (fold change, adropin/vehicle: ranging from 1.00 to 1.15, $P > 0.05$). Interestingly, we found that the hepatic malonyl-CoA level in adropin-treated DIO exhibited a strong trend towards decrease (nmole/g; adr.: 1.4 ± 0.1 vs. veh.: 2.5 ± 0.7). As malonyl-CoA is an allosteric inhibitor of CPT-1 [29], and liver is another key organ metabolizing fatty acids, adropin treatment might activate hepatic FAO, thus leading to an increase in fatty acid clearance from blood.

3.8. Adropin treatment did not alter phosphorylation of JNK and IKK kinase

Mitochondrial fatty acid overload may produce oxidative stress that impairs insulin signaling actions by activating c-Jun NH_2 terminal kinase (JNK) and inhibitor kappa B kinase (IKK) [30,66,67]. The JNK/IKK kinases inhibit insulin-induced tyrosine phosphorylation of insulin receptor substrates (IRS) [68]. In our studies, we measured the phosphorylation levels, surrogate markers of the enzymatic activity [69], of these two kinases. Adropin treatment did not affect the phosphorylation levels, as compared with the vehicle-treated DIO mice, which suggests that adropin actions did not impact the activity of JNK or IKK (Figure S5). These results are consistent with the finding (Figure S1A)

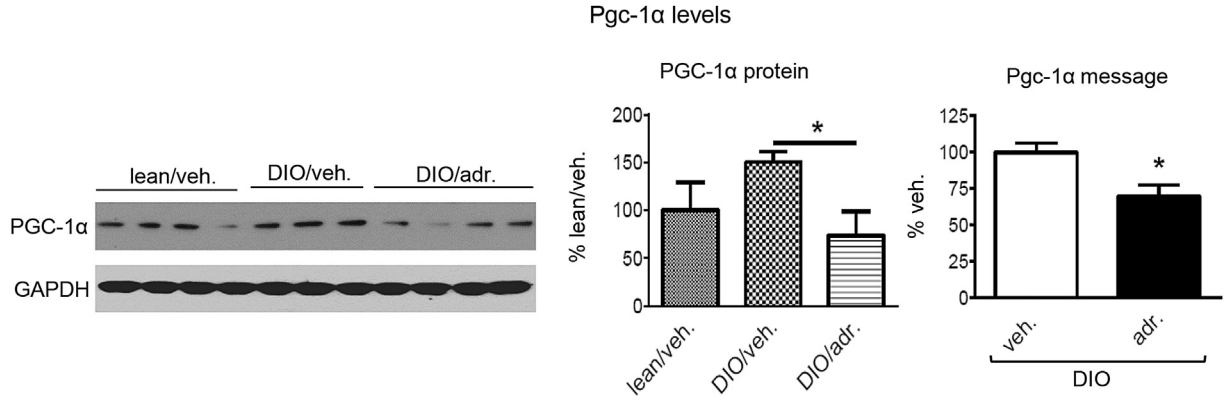

Figure 7: Adropin treatment decreased PGC-1α expression levels in the muscle of DIO mice. Shown are the levels of PGC-1α protein ($n = 3–4$) and mRNA ($n = 6$) in muscle. *, $P < 0.05$.

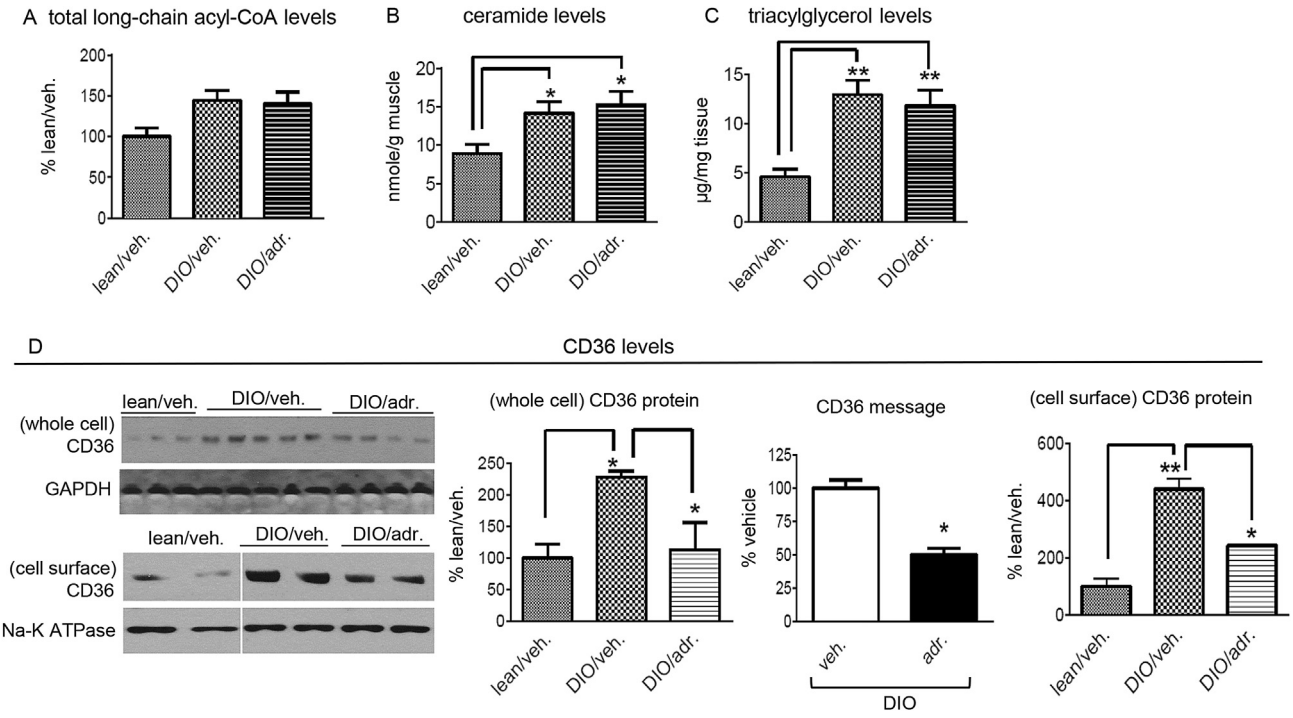

Figure 8: Adropin treatment did not alter intramuscular lipid intermediate levels in DIO mice. (A) Individual long-chain fatty acyl-CoA's levels in muscle were measured, and the sum of the individual acyl-CoA's was calculated as the total level. The assay was performed in two separate groups, and the average level of the "lean/veh." was set as "100%" ($n = 8–10$). (B) Ceramide levels in muscle ($n = 5–6$). (C) Triacylglycerol (TAG) levels in muscle ($n = 6–8$). (D) The levels of CD36 protein in the cell surface ($n = 3–5$), CD36 message ($n = 6$) and CD36 protein in whole muscle (two samples pooled, $n = 2$). *, $P < 0.05$; **, $P < 0.01$.

that adropin treatment did not restore the response of IRS1 phosphorylation upon insulin challenge.

3.9. Adropin treatment was associated with increased notch signaling in skeletal muscle

A recent report suggested that adropin retained in the plasma membrane modulates Notch1 signaling pathway [5]. We tested this hypothesis by measuring the expression levels of Hair and Enhancer of split (Hes), a prototypical target gene of Notch signaling [70]. In DIO mice, adropin$^{34-76}$ treatment increased *Hes1* mRNA level in muscle (Figure S6A), indicating stimulation of Notch signaling pathways. We also measured *Hes1* mRNA in skeletal muscle of adropin transgenic overexpression and knockout mice maintained on regular chow diet. The level of *Hes1* mRNA was increased in adropin overexpressing transgenic mice (Figure S6B), and was decreased in the adropin knockout mice (Figure S6C). These data are consistent with the previous report showing that overexpression of adropin in cultured cells upregulates *Hes1* mRNA level [5]. Moreover, Hes1 expression in the cerebellum was decreased in adropin knockout mice [5], which is also consistent with our findings. Here, our study using adropin$^{34-76}$ treatment indicates that circulating adropin may also interact with Notch signaling pathways in muscle.

4. DISCUSSION

4.1. Adropin$^{34-76}$ therapy enhanced oxidative glucose disposal while limiting fat oxidation

This report extends our recent findings on adropin's physiological role of regulating muscle substrate oxidation, investigating the metabolic actions of adropin treatment in DIO mouse muscle. Adropin$^{34-76}$ therapy reduced *Cpt1b* expression contributing to the inhibition of CPT-1B, and decreased Pdk4 expression contributing to the activation of PDH, in muscle of DIO mice. Furthermore, adropin treatment decreased Cd36 expression levels, with a potential consequence of reducing muscle fatty acid uptake. Associated with the reduced expressions of these proteins is the downregulation of transcriptional co-activator PGC-1α, a transcription co-activator that regulates the expression of *Cpt1b*, *Pdk4* and *Cd36* genes [58–61]. Thus, the downregulation of PGC-1α would lead to a reduction of its transcriptional activity, which could in part account for the suppressed expressions of the target genes.

The mechanisms underlying adropin-induced downregulation of PGC-1α are elusive. However, one potential mechanism may involve Notch1 signaling. Hes1, the canonical Notch target, acts as a transcriptional repressor, and physically binds to the promoter region of PGC-1α, thereby suppressing its expression [71]. In our studies, associated with repressing PGC-1αexpression, adropin treatment upregulated Hes1 expression. It follows that adropin action might inhibit PGC-1α expression in DIO muscle through activating Notch1 signaling pathway. How adropin alters notch signaling is not clear, while a direct physical interaction between adropin$^{34-76}$ and the membrane bound proteins that constitute the notch signaling pathway has likewise not been established. Future studies determining whether adropin physically interacts with the notch signaling network and how this interaction alters signaling are clearly needed.

In our previous report, adropin's actions induce hyperacetylation of PGC-1α protein (inhibiting the transcriptional activity) without altering its expression; a response that may involve downregulation of SIRT1 protein [3]. In the current study, SIRT1 protein levels in DIO mice were too low to be reliably detected. This finding is consistent with the

results of a previous study reporting that high-fat diet markedly reduces SIRT1 expression in muscle [72]. We nevertheless attempted measurements of nuclear SIRT deacetylase activity in DIO mice, finding no changes in response to adropin treatment (in AFU/min/μg protein; vehicle-treated: 2.4 ± 0.29, adropin-treated: 2.2 ± 0.47). Thus, in skeletal muscle of DIO mice, SIRT1 does not seem to be involved in adropin's action on PGC-1α. One interpretation for the lack of change in SIRT1 level is that basal levels of SIRT1 in DIO muscle are already very low, with no further reductions either elicited or detected in response to adropin treatment.

Adropin$^{34\text{-}76}$ treatment increased PDH activity in the muscle of DIO mice. Here, we discuss several mechanisms underlying this effect supported by our data. First, adropin's effect on PDK-4 expression is expected to play a role in the activation of PDH. Adropin treatment, likely through downregulating PGC-1α, decreased PDK4 expression which would then reduce its enzymatic activity. Moreover, adropin treatment increased the CoA/acetyl-CoA ratio, which allosterically inhibits PDK4 activity [3,29,73]. Together, the reduced PDK4 activity decreases the phosphorylation levels of the E1α subunit, increasing PDH activity. In addition, acetylation of E1α subunit is negatively associated with PDH enzymatic activity [37]. The decreased acetylation of the E1a subunit by adropin$^{34\text{-}76}$ thus provides another mechanism underlying the activation of PDH. Finally, the increase in the ratio of CoA/acetyl-CoA (by adropin treatment) would directly promote PDH activity and pyruvate oxidation [3,29].

4.2. Adropin$^{34\text{-}76}$ therapy improved mitochondrial function

A recent report proposed that mitochondrial fatty acid overload contributes to the development of diet-induced glucose intolerance and insulin resistance [30]. High-fat diet feeding augments muscle mitochondrial fatty acid uptake, resulting in an increased load of β-oxidative pathway [30,31]. In the presence of this overload, several adaptive metabolic responses were initiated, including upregulations of the capacity of β-oxidation and tricarboxylic acid (TCA) cycle [74]. These adaptive responses support an increased flux through β-oxidation pathway. However, the excessive β-oxidation can exceed the TCA cycle capacity, resulting in the accumulation of incompletely oxidized fatty acid intermediates [30,31]. In mitochondria, the elevation of incomplete FAO fosters a metabolic environment that favors sequestration of free CoA into acetyl-CoA [30,31], which ultimately results in a reduction of CoA/acetyl-CoA ratio. The decrease in CoA/acetyl-CoA has marked impacts on mitochondrial function, with one effect, as mentioned above, being the inhibition of PDH activity [30]. Here, our data demonstrated that adropin treatment reduced the elevated level of incomplete FAO in DIO muscle, which is likely a combined effect of the downregulation of CD36 and the reduction of CPT-1 activity. In turn, the resulting decrease in incomplete β-oxidation would augment the CoA/acetyl-CoA ratio, which would then attenuate the impairment of mitochondrial function of substrate oxidation associated with excessive β−oxidation.

Adropin$^{34\text{-}76}$ therapy may also have regulated the ratio of NAD^+ to NADH, which we speculate to provide an additional mechanism underlying the observed activation of PDH. Excessive β-oxidation in the DIO condition tends to reduce the ratio of NAD^+ to NADH in mitochondria, which would promote activation of PDK4 and inhibit PDH [30,75]. Moreover, a reduction in NAD^+ would also restrict SIRT3 activity, thus impacting the acetylation levels of mitochondrial proteins including the PDH E1α subunit [37]. By reducing CPT-1B activity in muscle, adropin treatment has the potential to reverse the above effects that are associated with the excessive β-oxidation, thereby promoting PDH activity.

Thus, our data support the hypothesis [30,32] that limiting muscle mitochondrial fatty acid overload may be an effective strategy to ameliorate mitochondrial dysfunction with respect to substrate oxidation. Indeed, a growing body of evidence is in line with our finding that the inhibition of CPT-1 activity can boost the diminished PDH activity under DIO condition. For example, treatment of DIO mice with the CPT-1B-selective inhibitor oxfenicine activates PDH in muscle [32]. In addition to the pharmacological intervention, raising the level of malonyl-CoA, a physiological inhibitor of CPT-1, has also been employed to inhibit CPT-1 activity and elevate the PDH activity or glucose oxidation. The malonyl-CoA decarboxylase (MCD) knockout mice that have an increased malonyl-CoA level exhibited a preferential oxidation of glucose over fatty acid [30]. In human skeletal muscle cells, silencing MCD (resulting in an increase in malonyl-CoA level) augments cellular glucose oxidation level [76].

As PDH plays the gate-keeping role in glucose oxidation pathway, the activation of PDH in muscle underlies the increased whole body carbohydrate oxidation following adropin treatment. Furthermore, consistent with a previous report [32], the increase in glucose oxidation in muscle can greatly enhance whole body glucose tolerance. The notion that PDH activity state *per se* impacts glucose homeostasis is supported by several findings. The oxfenicine-treated DIO mice exhibited an improvement of glucose tolerance, which is in part due to the activation of muscle PDH [32]. Pdk4-deficient mice exhibit increased PDH activity and glucose oxidation in muscle, and have enhanced glucose tolerance [77]. Moreover, treatment of hyperglycemic Zucker fatty rats with PDK isoform-selective inhibitors reduces blood glucose levels [77]. Finally, reduced PDH activity in muscle-specific carnitine acetyltransferase knockout mice compromises glucose tolerance [78]. In contrast, carnitine supplementation alleviates inhibition of PDH activity in the insulin resistant state, and improves glucose homeostasis [78].

4.3. Adropin$^{34\text{-}76}$ therapy enhanced insulin actions via a non-canonical pathway

Adropin$^{34\text{-}76}$ therapy enhanced muscle insulin signaling actions, an effect that would also be expected to significantly contribute to the improved glucose tolerance. Treatment of DIO mice with adropin increased insulin-stimulated cell surface GLUT4 expression, indicating a potential increase in muscle glucose uptake upon insulin. Associated with the enhanced response of GLUT4 are the augmented insulin-induced phosphorylations of Akt and AS160, two upstream mediators involved in GLUT4 translocation in insulin signaling pathways. Interestingly, adropin pretreatment did not increase insulin-induced IRS1 phosphorylation and PI-3K recruitment to IRS1, the canonical insulin intracellular signaling pathway [79]. This selective modulation of the distal segment of insulin signaling pathway is not unprecedented. One study reported amelioration of hyperglycemia associated with the enhanced insulin-induced responses of Akt and GLUT4 translocation, without changes in IRS1 phosphorylation [33]. In our studies, adropin treatment appears to sensitize Akt response to insulin by downregulating PTEN with a potential increase in the basal level of PIP3. Thus, although PI3K was not effectively recruited upon insulin stimulation in the adropin-treated DIO mice, the inhibition of PTEN may raise the level of PIP_3 above a threshold required for triggering the insulin-induced Akt phosphorylation and activation. Mechanistically, the Notch signaling might mediate the effect of adropin treatment on PTEN expression. Activation of Notch signaling can exert an inhibitory effect on Pten expression [80,81], which is mediated by Hes1 that binds to the regulatory sequence in the promoter region in *Pten* gene [80].

The view of improving insulin sensitivity and glucose homeostasis by restricting mitochondrial fatty acid uptake seems to contradict the traditional idea [82] that promotion of mitochondrial FAO alleviates insulin resistance. The increase in mitochondrial FAO is generally believed to have the ability of lowering the level of cytosolic bioactive lipid intermediates, thereby enhancing insulin sensitivity [64,82]. This argument has been supported by the finding that activation of muscle CPT-1 alleviates insulin resistance in high fat diet-fed animals [82]. In that report, CPT-1 activation increased FAO level, and reduced the amounts of intramuscular lipid intermediates [82]. In contrast, in the current report, the inhibition of CPT-1 by adropin treatment did not result in the elevation of the cellular bioactive lipid levels, which seems to be paradoxical to the changes found in the CPT-1 overexpression study [82]. In our studies, adropin treatment reduced whole cellular as well as cell surface Cd36 expression levels, and these changes indicates a potential reduction of muscle fatty acid uptake [32]. We propose that the downregulation of CD36 would play a key role in preventing the cellular levels of lipid intermediates from rising in response to adropin treatment. Interestingly, the similar findings have been demonstrated in some other reports employing inhibition of CPT-1 as an approach to improve glucose homeostasis. Oxfenicine treatment also results in a downregulation of plasma membrane level of CD36 [32], and MCD silencing in human muscle cells is associated with a reduced expression of fatty acid transport protein (Fatp) and a decreased palmitate uptake [76]. On the other hand, the CPT-1 overexpression study [82] also does not contradict the hypothesis that preventing mitochondrial overload has beneficial effects on glucose tolerance and insulin sensitivity. We speculate that the activation of muscle CPT-1 in that study did not elevate mitochondrial fatty acid uptake to a level that β-oxidation exceeds the capacity of the TCA cycle. As a result, the incomplete oxidation had not been significantly developed, and consequently, the CoA/acetyl-CoA ratio was maintained, leaving no major effect on the activity of PDH. Indeed, this prediction is supported by the finding that the levels of the incompletely oxidized fatty acid intermediates were not significantly increased following the overexpression of CPT-1 [82].

Taken together, these results demonstrate that the coordinated actions on metabolic pathways produce different physiological outcomes from uncoordinated or isolated actions. To further support this argument, the paradoxical effect of muscle-specific overexpression of PGC-1α on insulin sensitivity provides another example [83]. In this study, the increased expression of PGC-1α in muscle unexpectedly resulted in insulin resistance [83]. It should be particularly noted that, in parallel with the increased mitochondrial oxidative capacity, Cd36 levels were also elevated by PGC-1α overexpression [83]. The upregulation of Cd36 would facilitate fatty acid uptake, which may lead to accumulation of toxic lipid intermediates, and thus the impairment of insulin sensitivity [83]. However, adropin treatment appears to initiate coordinated actions on fuel-handling proteins, which maintains intramuscular lipid levels while preserves insulin control of glucose metabolism. In the current and previous reports, we have focused on the metabolic effects of adropin on skeletal muscle. Besides muscle, adropin also regulates endothelial function [6]. Notably, adropin treatment induces activation of endothelial nitric oxide synthase (eNOS) that produces nitric oxide, a critical endogenous vasodilator [6,84]. In our studies, the observed improvements of glucose and insulin tolerance may stem partly from the potential effect of adropin on vasodilation in the muscle. The consequent enhancement of blood perfusion can increase glucose availability, which could augment glucose metabolism.

4.4. Summary

The current study provides a molecular basis for the improvements in glucose homeostasis that are observed with adropin treatment. Our data suggest that skeletal muscle is a major organ target in mediating these effects, although actions involving other insulin-target organs are possible and further investigation is clearly warranted. These data support the notion that adropin may be a promising drug target in developing treatments against diet-induced dysregulation of glucose homeostasis and insulin resistance.

5. AUTHOR CONTRIBUTIONS

S.G. and A.A.B. contributed to the study concept and design, data analysis and interpretation, and writing of the manuscript. R.P.M. and M.W.H. contributed to the collection of data, data interpretation, and reviewed the manuscript. Q.Z. and G.D.L. contributed with technical assistance and data collection and reviewed the manuscript. S.G. and A.A.B. are the guarantors of this work and, as such, had full access to all the data in the study and take responsibility for the integrity and accuracy of data analysis.

ACKNOWLEDGMENTS

This work was supported by a Proof of Principle Award from Novo Nordisk's Diabetes Innovation Award Program (to A.A.B.), the National Institute of Diabetes and Digestive and Kidney Diseases (R01-DK-078765 to M.W.H), the American Diabetes Association (1-13-CE-16 to M.W.H. and 7-08-RA-16 to A.A.B.) and a grant from the Canadian Diabetes Association (to G.D.L.).

CONFLICT OF INTEREST

A.A.B. was supported by a Proof of Principle Award from Novo Nordisk's Diabetes Innovation Award Program. No other potential conflicts of interest relevant to this article were reported.

APPENDIX A. SUPPLEMENTARY DATA

Supplementary data related to this article can be found at http://dx.doi.org/10.1016/j.molmet.2015.01.005

REFERENCES

[1] Goetze, J.P., Albrethsen, J., 2014. Adropin: a new regulatory peptide in cardiovascular endocrinology. Regulatory Peptides 190–191:41–42.

[2] Aydin, S., 2014. Three new players in energy regulation: preptin, adropin and irisin. Peptides 56:94–110.

[3] Gao, S., McMillan, R.P., Jacas, J., Zhu, Q., Li, X., Kumar, G.K., et al., 2014. Regulation of substrate oxidation preferences in muscle by the peptide hormone adropin. Diabetes 63(10):3242–3452.

[4] Kumar, K.G., Trevaskis, J.L., Lam, D.D., Sutton, G.M., Koza, R.A., Chouljenko, V.N., et al., 2008. Identification of adropin as a secreted factor linking dietary macronutrient intake with energy homeostasis and lipid metabolism. Cell Metabolism 8:468–481.

[5] Wong, C.-M., Wang, Y., Lee, J.T.H., Huang, Z., Wu, D., Xu, A., et al., 2014. Adropin is a brain membrane-bound protein regulating physical activity via the NB-3/Notch signaling pathway in mice. Journal of Biological Chemistry 289: 25976–25986.

[6] Lovren, F., Pan, Y., Quan, A., Singh, K.K., Shukla, P.C., Gupta, M., et al., 2010. Adropin is a novel regulator of endothelial function. Circulation 122:S185–S192.

[7] Yu, H.Y., Zhao, P., Wu, M.C., Liu, J., Yin, W., 2014. Serum adropin levels are decreased in patients with acute myocardial infarction. Regulatory Peptides 190–191:46–49.
[8] Yildirim, B., Celik, O., Aydin, S., 2014. Adropin: a key component and potential gatekeeper of metabolic disturbances in policystic ovarian syndrome. Clinical and Experimental Obstetrics & Gynecology 41:310–312.
[9] Wu, L., Fang, J., Chen, L., Zhao, Z., Luo, Y., Lin, C., et al., 2014. Low serum adropin is associated with coronary atherosclerosis in type 2 diabetic and non-diabetic patients. Clinical Chemistry and Laboratory Medicine: CCLM/FESCC 52:751–758.
[10] St-Onge, M.P., Shechter, A., Shlisky, J., Tam, C.S., Gao, S., Ravussin, E., et al., 2014. Fasting plasma adropin concentrations correlate with fat consumption in human females. Obesity 22:1056–1063.
[11] Sayin, O., Tokgoz, Y., Arslan, N., 2014. Investigation of adropin and leptin levels in pediatric obesity-related nonalcoholic fatty liver disease. Journal of Pediatric Endocrinology & Metabolism: JPEM 27:479–484.
[12] Qiu, X., He, J.R., Zhao, M.G., Kuang, Y.S., Xu, S.Q., Zhang, H.Z., et al., 2014. Relationship between human cord blood adropin levels and fetal growth. Peptides 52:19–22.
[13] Demircelik, B., Cakmak, M., Nazli, Y., Gurel, O.M., Akkaya, N., Cetin, M., et al., 2014. Adropin: a new marker for predicting late saphenous vein graft disease after coronary artery bypass grafting. Clinical and Investigative Medicine. Medecine clinique et experimentale 37:E338.
[14] Aydin, S., Kuloglu, T., Aydin, S., Kalayci, M., Yilmaz, M., Cakmak, T., et al., 2014. Elevated adropin: a candidate diagnostic marker for myocardial infarction in conjunction with troponin-I. Peptides 58:91–97.
[15] Topuz, M., Celik, A., Aslantas, T., Demir, A.K., Aydin, S., Aydin, S., 2013. Plasma adropin levels predict endothelial dysfunction like flow-mediated dilatation in patients with type 2 diabetes mellitus. Journal of Investigative Medicine: The Official Publication of the American Federation for Clinical Research 61:1161–1164.
[16] Gozal, D., Kheirandish-Gozal, L., Bhattacharjee, R., Molero-Ramirez, H., Tan, H.L., Bandla, H.P., 2013. Circulating adropin concentrations in pediatric obstructive sleep apnea: potential relevance to endothelial function. The Journal of Pediatrics 163:1122–1126.
[17] Celik, E., Yilmaz, E., Celik, O., Ulas, M., Turkcuoglu, I., Karaer, A., et al., 2013. Maternal and fetal adropin levels in gestational diabetes mellitus. Journal of Perinatal Medicine 41:375–380.
[18] Celik, A., Balin, M., Kobat, M.A., Erdem, K., Baydas, A., Bulut, M., et al., 2013. Deficiency of a new protein associated with cardiac syndrome X; called adropin. Cardiovascular Therapeutics 31:174–178.
[19] Aydin, S., Kuloglu, T., Aydin, S., Eren, M.N., Yilmaz, M., Kalayci, M., et al., 2013. Expression of adropin in rat brain, cerebellum, kidneys, heart, liver, and pancreas in streptozotocin-induced diabetes. Molecular and Cellular Biochemistry 380:73–81.
[20] Ganesh Kumar, K., Zhang, J., Gao, S., Rossi, J., McGuinness, O.P., Halem, H.H., et al., 2012. Adropin deficiency is associated with increased adiposity and insulin resistance. Obesity 20:1394–1402.
[21] Butler, A.A., Tam, C.S., Stanhope, K.L., Wolfe, B.M., Ali, M.R., O'Keeffe, M., et al., 2012. Low circulating adropin concentrations with obesity and aging correlate with risk factors for metabolic disease and increase after gastric bypass surgery in humans. The Journal of Clinical Endocrinology & Metabolism 97:3783–3791.
[22] Lian, W., Gu, X., Qin, Y., Zheng, X., 2011. Elevated plasma levels of adropin in heart failure patients. Internal Medicine 50:1523–1527.
[23] Bremer, A.A., Stanhope, K.L., Graham, J.L., Cummings, B.P., Ampah, S.B., Saville, B.R., et al., 2014. Fish oil supplementation ameliorates fructose-induced hypertriglyceridemia and insulin resistance in adult male rhesus macaques. The Journal of Nutrition 144:5–11.
[24] Kuhla, A., Hahn, S., Butschkau, A., Lange, S., Wree, A., Vollmar, B., 2014. Lifelong caloric restriction reprograms hepatic fat metabolism in mice. The Journals of Gerontology. Series A, Biological Sciences and Medical Sciences 69:915–922.
[25] Partridge, C.G., Fawcett, G.L., Wang, B., Semenkovich, C.F., Cheverud, J.M., 2014. The effect of dietary fat intake on hepatic gene expression in LG/J AND SM/J mice. BMC Genomics 15:99.
[26] McGarry, J.D., Brown, N.F., 1997. The mitochondrial carnitine palmitoyltransferase system. From concept to molecular analysis. European Journal of Biochemistry 244:1–14.
[27] Otero, Y.F., Stafford, J.M., McGuinness, O.P., 2014. Pathway-selective insulin resistance and metabolic disease: the importance of nutrient flux. The Journal of Biological Chemistry 289:20462–20469.
[28] Randle, P.J., Garland, P.B., Hales, C.N., Newsholme, E.A., 1963. The glucose fatty-acid cycle. Its role in insulin sensitivity and the metabolic disturbances of diabetes mellitus. Lancet 1:785–789.
[29] Hue, L., Taegtmeyer, H., 2009. The Randle cycle revisited: a new head for an old hat. American Journal of Physiology. Endocrinology and Metabolism 297: E578–E591.
[30] Koves, T.R., Ussher, J.R., Noland, R.C., Slentz, D., Mosedale, M., Ilkayeva, O., et al., 2008. Mitochondrial overload and incomplete fatty acid oxidation contribute to skeletal muscle insulin resistance. Cell Metabolism 7:45–56.
[31] Muoio, D.M., Newgard, C.B., 2008. Fatty acid oxidation and insulin action: when less is more. Diabetes 57:1455–1456.
[32] Keung, W., Ussher, J.R., Jaswal, J.S., Raubenheimer, M., Lam, V.H., Wagg, C.S., et al., 2013. Inhibition of carnitine palmitoyltransferase-1 activity alleviates insulin resistance in diet-induced obese mice. Diabetes 62:711–720.
[33] Lusk, G., 1924. Animal calorimetry: twenty-fourth paper. Analysis of the oxidation of mixtures of carbohydrate and fat. Journal of Biological Chemistry 59:41–42.
[34] Araujo, E.P., De Souza, C.T., Gasparetti, A.L., Ueno, M., Boschero, A.C., Saad, M.J., et al., 2005. Short-term in vivo inhibition of insulin receptor substrate-1 expression leads to insulin resistance, hyperinsulinemia, and increased adiposity. Endocrinology 146:1428–1437.
[35] Hulver, M.W., Berggren, J.R., Cortright, R.N., Dudek, R.W., Thompson, R.P., Pories, W.J., et al., 2003. Skeletal muscle lipid metabolism with obesity.
[36] Morillas, M., Gomez-Puertas, P., Roca, R., Serra, D., Asins, G., Valencia, A., et al., 2001. Structural model of the catalytic core of carnitine palmitoyltransferase I and carnitine octanoyltransferase (COT): mutation of CPT I histidine 473 and alanine 381 and COT alanine 238 impairs the catalytic activity. The Journal of Biological Chemistry 276:45001–45008.
[37] Jing, E., O'Neill, B.T., Rardin, M.J., Kleinridders, A., Ilkeyeva, O.R., Ussar, S., et al., 2013. Sirt3 regulates metabolic flexibility of skeletal muscle through reversible enzymatic deacetylation. Diabetes 62(10):3404–3417.
[38] Welsh, G.I., Hers, I., Berwick, D.C., Dell, G., Wherlock, M., Birkin, R., et al., 2005. Role of protein kinase B in insulin-regulated glucose uptake. Biochemical Society Transactions 33:346–349.
[39] Cho, H., Mu, J., Kim, J.K., Thorvaldsen, J.L., Chu, Q., Crenshaw 3rd, E.B., et al., 2001. Insulin resistance and a diabetes mellitus-like syndrome in mice lacking the protein kinase Akt2 (PKB beta). Science 292:1728–1731.
[40] Kruszynska, Y.T., Worrall, D.S., Ofrecio, J., Frias, J.P., Macaraeg, G., Olefsky, J.M., 2002. Fatty acid-induced insulin resistance: decreased muscle PI3K activation but unchanged Akt phosphorylation. The Journal of Clinical Endocrinology & Metabolism 87:226–234.
[41] Morino, K., Neschen, S., Bilz, S., Sono, S., Tsirigotis, D., Reznick, R.M., et al., 2008. Muscle-specific IRS-1 Ser→Ala transgenic mice are protected from fat-induced insulin resistance in skeletal muscle. Diabetes 57:2644–2651.
[42] Kramer, H.F., Witczak, C.A., Taylor, E.B., Fujii, N., Hirshman, M.F., Goodyear, L.J., 2006. AS160 regulates insulin- and contraction-stimulated glucose uptake in mouse skeletal muscle. The Journal of Biological Chemistry 281:31478–31485.

[43] Kramer, H.F., Witczak, C.A., Fujii, N., Jessen, N., Taylor, E.B., Arnolds, D.E., et al., 2006. Distinct signals regulate AS160 phosphorylation in response to insulin, AICAR, and contraction in mouse skeletal muscle. Diabetes 55:2067–2076.

[44] Funai, K., Song, H., Yin, L., Lodhi, I.J., Wei, X., Yoshino, J., et al., 2013. Muscle lipogenesis balances insulin sensitivity and strength through calcium signaling. The Journal of Clinical Investigation 123(3):1229–1240.

[45] Zisman, A., Peroni, O.D., Abel, E.D., Michael, M.D., Mauvais-Jarvis, F., Lowell, B.B., et al., 2000. Targeted disruption of the glucose transporter 4 selectively in muscle causes insulin resistance and glucose intolerance. Nature Medicine 6:924–928.

[46] Saltiel, A.R., Kahn, C.R., 2001. Insulin signalling and the regulation of glucose and lipid metabolism. Nature 414:799–806.

[47] Anai, M., Funaki, M., Ogihara, T., Kanda, A., Onishi, Y., Sakoda, H., et al., 1999. Enhanced insulin-stimulated activation of phosphatidylinositol 3-kinase in the liver of high-fat-fed rats. Diabetes 48:158–169.

[48] Hers, I., Vincent, E.E., Tavare, J.M., 2011. Akt signalling in health and disease. Cellular Signalling 23:1515–1527.

[49] Holness, M.J., Sugden, M.C., 2003. Regulation of pyruvate dehydrogenase complex activity by reversible phosphorylation. Biochemical Society Transactions 31:1143–1151.

[50] Sugden, M.C., Holness, M.J., 2003. Recent advances in mechanisms regulating glucose oxidation at the level of the pyruvate dehydrogenase complex by PDKs. American Journal of Physiology - Endocrinology and Metabolism 284: E855–E862.

[51] Holness, M.J., Kraus, A., Harris, R.A., Sugden, M.C., 2000. Targeted upregulation of pyruvate dehydrogenase kinase (PDK)-4 in slow-twitch skeletal muscle underlies the stable modification of the regulatory characteristics of PDK induced by high-fat feeding. Diabetes 49:775–781.

[52] Lombard, D.B., Alt, F.W., Cheng, H.-L., Bunkenborg, J., Streeper, R.S., Mostoslavsky, R., et al., 2007. Mammalian Sir2 Homolog SIRT3 regulates global mitochondrial lysine acetylation. Molecular and Cellular Biology 27: 8807–8814.

[53] Palacios, O.M., Carmona, J.J., Michan, S., Chen, K.Y., Manabe, Y., Ward 3rd, J.L., et al., 2009. Diet and exercise signals regulate SIRT3 and activate AMPK and PGC-1alpha in skeletal muscle. Aging 1:771–783.

[54] Rardin, M.J., Wiley, S.E., Naviaux, R.K., Murphy, A.N., Dixon, J.E., 2009. Monitoring phosphorylation of the pyruvate dehydrogenase complex. Analytical Biochemistry 389:157–164.

[55] Sugden, M.C., Howard, R.M., Munday, M.R., Holness, M.J., 1993. Mechanisms involved in the coordinate regulation of strategic enzymes of glucose metabolism. Advances in Enzyme Regulation 33:71–95.

[56] Bowker-Kinley, M., Davis, W., Wu, P., HARRIS, R., POPOV, K., 1998. Evidence for existence of tissue-specific regulation of the mammalian pyruvate dehydrogenase complex. The Biochemical Journal 329:191–196.

[57] Lin, J., Handschin, C., Spiegelman, B.M., 2005. Metabolic control through the PGC-1 family of transcription coactivators. Cell Metabolism 1:361–370.

[58] Wende, A.R., Huss, J.M., Schaeffer, P.J., Giguere, V., Kelly, D.P., 2005. PGC-1alpha coactivates PDK4 gene expression via the orphan nuclear receptor ERRalpha: a mechanism for transcriptional control of muscle glucose metabolism. Molecular and Cellular Biology 25:10684–10694.

[59] Moore, M.L., Park, E.A., McMillin, J.B., 2003. Upstream stimulatory factor represses the induction of carnitine palmitoyltransferase-Ibeta expression by PGC-1. The Journal of Biological Chemistry 278:17263–17268.

[60] Wende, A.R., Schaeffer, P.J., Parker, G.J., Zechner, C., Han, D.-H., Chen, M.M., et al., 2007. A role for the transcriptional coactivator PGC-1α in muscle refueling. Journal of Biological Chemistry 282:36642–36651.

[61] Benton, C.R., Nickerson, J.G., Lally, J., Han, X.-X., Holloway, G.P., Glatz, J.F.C., et al., 2008. Modest PGC-1α overexpression in muscle in vivo is sufficient to increase insulin sensitivity and palmitate oxidation in subsarcolemmal, not intermyofibrillar, mitochondria. The Journal of Biological Chemistry 283: 4228–4240.

[62] Larsen, S., Nielsen, J., Hansen, C.N., Nielsen, L.B., Wibrand, F., Stride, N., et al., 2012. Biomarkers of mitochondrial content in skeletal muscle of healthy young human subjects. The Journal of Physiology 590:3349–3360.

[63] Ekstrand, M.I., Falkenberg, M., Rantanen, A., Park, C.B., Gaspari, M., Hultenby, K., et al., 2004. Mitochondrial transcription factor A regulates mtDNA copy number in mammals. Human Molecular Genetics 13:935–944.

[64] Kim, J.K., Fillmore, J.J., Chen, Y., Yu, C., Moore, I.K., Pypaert, M., et al., 2001. Tissue-specific overexpression of lipoprotein lipase causes tissue-specific insulin resistance. Proceedings of the National Academy of Sciences of the United States of America 98:7522–7527.

[65] Goudriaan, J.R., den Boer, M.A.M., Rensen, P.C.N., Febbraio, M., Kuipers, F., Romijn, J.A., et al., 2005. CD36 deficiency in mice impairs lipoprotein lipase-mediated triglyceride clearance. Journal of Lipid Research 46:2175–2181.

[66] Yuan, M., Konstantopoulos, N., Lee, J., Hansen, L., Li, Z.W., Karin, M., et al., 2001. Reversal of obesity- and diet-induced insulin resistance with salicylates or targeted disruption of Ikkbeta. Science 293:1673–1677.

[67] Hirosumi, J., Tuncman, G., Chang, L., Gorgun, C.Z., Uysal, K.T., Maeda, K., et al., 2002. A central role for JNK in obesity and insulin resistance. Nature 420:333–336.

[68] Boura-Halfon, S., Zick, Y., 2009. Phosphorylation of IRS proteins, insulin action, and insulin resistance. American Journal of Physiology – Endocrinology and Metabolism 296:E581–E591.

[69] Yaspelkis 3rd, B.B., Kvasha, I.A., Figueroa, T.Y., 2009. High-fat feeding increases insulin receptor and IRS-1 coimmunoprecipitation with SOCS-3, IKKalpha/beta phosphorylation and decreases PI-3 kinase activity in muscle. The American Journal of Physiology - Regulatory, Integrative and Comparative Physiology 296:R1709–R1715.

[70] Jarriault, S., Le Bail, O., Hirsinger, E., Pourquie, O., Logeat, F., Strong, C.F., et al., 1998. Delta-1 activation of notch-1 signaling results in HES-1 transactivation. Molecular and Cellular Biology 18:7423–7431.

[71] Bi, P., Shan, T., Liu, W., Yue, F., Yang, X., Liang, X.-R., et al., 2014. Inhibition of notch signaling promotes browning of white adipose tissue and ameliorates obesity. Nature Medicine 20:911–918.

[72] Sun, C., Zhang, F., Ge, X., Yan, T., Chen, X., Shi, X., et al., 2007. SIRT1 improves insulin sensitivity under insulin-resistant conditions by repressing PTP1B. Cell Metabolism 6:307–319.

[73] Pettit, F.H., Pelley, J.W., Reed, L.J., 1975. Regulation of pyruvate dehydrogenase kinase and phosphatase by acetyl-CoA/CoA and NADH/NAD ratios. Biochemical and Biophysical Research Communications 65:575–582.

[74] Turner, N., Bruce, C.R., Beale, S.M., Hoehn, K.L., So, T., Rolph, M.S., et al., 2007. Excess lipid availability increases mitochondrial fatty acid oxidative capacity in muscle: evidence against a role for reduced fatty acid oxidation in lipid-induced insulin resistance in rodents. Diabetes 56:2085–2092.

[75] Crewe, C., Kinter, M., Szweda, L.I., 2013. Rapid inhibition of pyruvate dehydrogenase: an initiating event in high dietary fat-induced loss of metabolic flexibility in the heart. PLoS ONE 8:e77280.

[76] Bouzakri, K., Austin, R., Rune, A., Lassman, M.E., Garcia-Roves, P.M., Berger, J.P., et al., 2008. Malonyl CoenzymeA decarboxylase regulates lipid and glucose metabolism in human skeletal muscle. Diabetes 57:1508–1516.

[77] Jeoung, N.H., Harris, R.A., 2008. Pyruvate dehydrogenase kinase-4 deficiency lowers blood glucose and improves glucose tolerance in diet-induced obese mice. American Journal of Physiology. Endocrinology and Metabolism 295:E46–E54.

[78] Muoio, D.M., Noland, R.C., Kovalik, J.P., Seiler, S.E., Davies, M.N., DeBalsi, K.L., et al., 2012. Muscle-specific deletion of carnitine acetyltransferase compromises glucose tolerance and metabolic flexibility. Cell Metabolism 15:764–777.

[79] Brüning, J.C., Michael, M.D., Winnay, J.N., Hayashi, T., Hörsch, D., Accili, D., et al., 1998. A muscle-specific insulin receptor knockout exhibits features of

the metabolic syndrome of NIDDM without altering glucose tolerance. Molecular Cell 2:559–569.

[80] Palomero, T., Sulis, M.L., Cortina, M., Real, P.J., Barnes, K., Ciofani, M., et al., 2007. Mutational loss of PTEN induces resistance to NOTCH1 inhibition in T-cell leukemia. Nature Medicine 13:1203–1210.

[81] Wong, G.W., Knowles, G.C., Mak, T.W., Ferrando, A.A., Zuniga-Pflucker, J.C., 2012. HES1 opposes a PTEN-dependent check on survival, differentiation, and proliferation of TCRbeta-selected mouse thymocytes. Blood 120:1439–1448.

[82] Bruce, C.R., Hoy, A.J., Turner, N., Watt, M.J., Allen, T.L., Carpenter, K., et al., 2009. Overexpression of carnitine palmitoyltransferase-1 in skeletal muscle is sufficient to enhance fatty acid oxidation and improve high-fat diet-induced insulin resistance. Diabetes 58:550–558.

[83] Choi, C.S., Befroy, D.E., Codella, R., Kim, S., Reznick, R.M., Hwang, Y.J., et al., 2008. Paradoxical effects of increased expression of PGC-1alpha on muscle mitochondrial function and insulin-stimulated muscle glucose metabolism. Proceedings of the National Academy of Sciences of the United States of America 105:19926–19931.

[84] Forstermann, U., Closs, E.I., Pollock, J.S., Nakane, M., Schwarz, P., Gath, I., et al., 1994. Nitric oxide synthase isozymes. Characterization, purification, molecular cloning, and functions. Hypertension 23:1121–1131.

